IOPscience iopscience.iop.org

Home Search Collections Journals About Contact us My IOPscience

A study of nanostructure assemblies and guest-host interactions in sodium zeolite-Y using ^{23}Na double-rotation NMR

This article has been downloaded from IOPscience. Please scroll down to see the full text article.

1991 Nanotechnology 2 182

(http://iopscience.iop.org/0957-4484/2/4/003)

View the table of contents for this issue, or go to the journal homepage for more

Download details:
IP Address: 128.32.151.37
The article was downloaded on 19/04/2013 at 21:12

Please note that terms and conditions apply.

Nanotechnology 2 (1991) 182–186 Printed in the UK

A study of nanostructure assemblies and guest–host interactions in sodium zeolite–Y using ^{23}Na double-rotation NMR

Raz Jelinek†, Alexander Pines†§, Saim Özkar‡‖ and Geoffrey A Ozin‡

†Materials Sciences Division, Lawrence Berkeley Laboratory and Department of Chemistry, University of California, Berkeley, CA 94720, USA
‡Advanced Zeolite Materials Science Group, Lash Miller Chemical Laboratories, University of Toronto, 80 St. George Street, Toronto, Ontario, Canada M5S 1A1

Received 9 November 1991, accepted for publication 2 April 1992

Abstract. ^{23}Na double-rotation NMR (DOR) spectroscopy provides details on site-specific adsorption of various molecular guests within the nanometer-dimension void spaces of sodium zeolite-Y. Anchoring of hexacarbonyl metal(0) precursors, as well as their molecular metal oxide photooxidation products, to specific extraframework sodium cation sites, is readily detected by ^{23}Na DOR. Loading-dependent chemical shifts and line-shape alterations yield useful information on the structure, bonding and organization of the guests within the zeolite host lattice.

1. Introduction

Quantum confined semiconductor structures offer diverse technological and commercial opportunities in fields such as electronics, photonics and optoelectronics [1]. Interest in the properties and applications of uniform semiconductor arrays having zero-dimensional ['quantum dots'], one-dimensional ['quantum wires'], two-dimensional ['quantum wells'] and three-dimensional ['quantum supralattice'] quantum confinement has grown. A major challenge in this burgeoning field is the ability to control the arrangement of the atomic components of bulk semiconductors into well defined and organized nanostructures. Various synthetic techniques have been developed for achieving that goal, among them molecular beam epitaxy (MBE) and metal–organic chemical vapor deposition (MOCVD) [2], jet expansion [3], extraction through polymeric solutions [4], lipid membranes [5] and others. Recently, there has been growing interest in the use of porous materials such as zeolites as possible hosts for the fabrication of nanosize particles [6]. The uniform crystalline structure and nanometer-dimension channel and cavity spaces of these materials can be advantageously used for the self-assembly of the atomic constituents of bulk semiconductors into aggregates having precisely defined size and shape inside the zeolite lattice.

§ To whom correspondence should be addressed.
‖ On leave from the Chemistry Department, Middle East Technical University, Ankara, Turkey, 06531.

A crucial requirement for further progress in this field of 'intrazeolite nanotechnology', is the accurate and unambiguous structural determination of the constructed materials. Electron microscopy and various spectroscopy and diffraction techniques are employed for studying surfaces, thin films, interfaces, and microcrystalline materials. Single-crystal and Rietveld powder x-ray diffraction methods are pivotal in providing atomically precise structural details of solids that display long-range order. Solid-state nuclear magnetic resonance (NMR) on the other hand can yield invaluable information about the structure and configuration of atomic, ionic, cluster and molecular species in materials having both long- and short-range order like zeolites and molecular sieves.

This work concentrates on the application of high-resolution solid-state NMR, using the newly developed double-rotation (DOR) technique [7], in probing intimate structural details of zeolite 'guest–host' systems. In particular we investigate the intrazeolite photooxidation of hexacarbonyl molybdenum(0) and tungsten(0) precursors to yield the respective metal(VI) oxides.

2. Results and discussion

2.1. Intrazeolite molecular metal oxides of molybdenum and tungsten

The $Na_{56}Y$ $[Y = (AlO_2)_{56}(SiO_2)_{136}\cdot H_2O]$ zeolite framework is composed of a regular array of intercon-

0957-4484/91/04182+05 $3.50 © 1991 IOP Publishing Ltd

nected α cages as shown schematically in figure 1. The discrete, molecular size dimensions of the cavities thus offer the possibility of fabricating organized assemblies of atomic, molecular, and cluster guests using the zeolite framework as a 'template'. Extraframework charge-balancing sodium cations are distributed among four different sites within the zeolite lattice: site I in the hexagonal prism, I′ inside the sodalite cage, and sites II and III in the 13 Å wide α cage [8]. Distinct ^{23}Na DOR signals from the sodium environments within the zeolite framework were recently identified in our laboratory [9]; this development offers a direct probe of adsorption phenomena, anchoring interactions, structures and chemical and dynamical processes within the zeolite cavities, using solid-state ^{23}Na NMR.

A recent example of a controlled intrazeolitic reaction is the photooxidation of hexacarbonylmetal(0) complexes with dioxygen [10]. The reaction is carried out entirely within the α cages of $Na_{56}Y$ zeolite, yielding encapsulated metal(VI) oxides according to the following reaction stoichiometry:

$$m\{M(CO)_6\} - Na_{56}Y + \tfrac{9}{2}nO_2 \xrightarrow{h\nu} m\{MO_3\} - Na_{56}Y + 6nCO_2$$

where M = Mo, W, and $0 \leqslant m \leqslant 16$.

The above reaction is clean and quantitative and leads to molecular MoO_3 and WO_3 semiconductor species. An especially noteworthy feature of these intrazeolite metal oxides is the inability to control their oxygen stoichiometries through vacuum thermal reductive elimination of O_2, according to the following reactions:

$$n\{WO_3\}-Na_{56}Y \xrightarrow{300^\circ C} n\{WO_{2.5}\}-Na_{56}Y \xrightarrow{400^\circ C} n\{WO_2\}-Na_{56}Y$$

and

$$n\{MoO_3\}-Na_{56}Y \xrightarrow{400^\circ C} n\{MoO_2\}-Na_{56}Y.$$

These processes can be quantitatively reversed by exposing the reduced samples to O_2 gas at 400°C and 300°C, respectively. Thus, one can achieve an effect similar to 'n-doping' of the bulk semiconductor material [11]. In addition, it was demonstrated that the HOMO–LUMO (VB–CB) energy gaps in the $16\{WO_3\}-M_{56}Y$ series, where M = H, Li, Na, K, Rb and Cs, can be tuned in a systematic way by altering the α-cage electric fields associated with the extraframework cations [11].

The physical dimensions of the window and void spaces of the sodium zeolite Y host lattice constrain both the $M(CO)_6$ precursors and MO_3 products to the diamond network of essentially spherical 13 Å α cages. A multiprong analytical approach—diffraction, spectroscopy, microscopy, thermal and chemical—has been

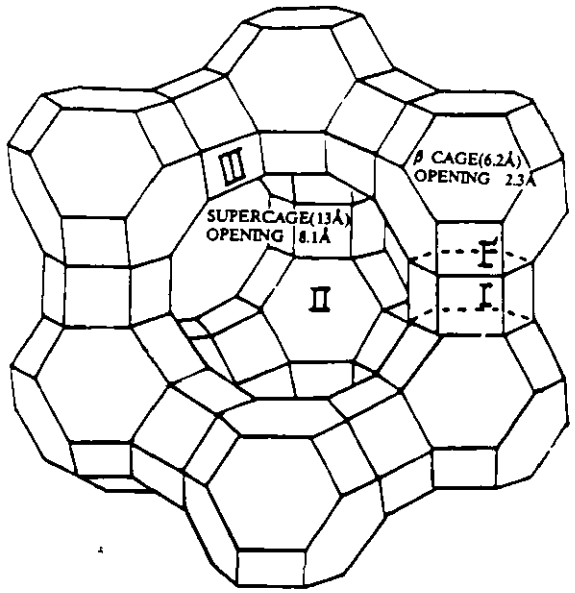

Figure 1. A schematic drawing of part of the unit cell of $Na_{56}Y$ zeolite showing the α cage. I, I′, II and III indicate extraframework charge balancing Na^+ cation sites [8].

applied to all of the aforementioned precursors and products [10–13] in order to elucidate their structures and some of their properties. The proposed structures and anchoring geometries of the molybdenum and tungsten $16\{MO_{3-x}\}-Na_{56}Y$ series inside the Y-zeolite α cage is depicted in figure 2. From inspection of the figures, one notices that a ubiquitous feature of all $M(CO)_6$ and MO_{3-x} intrazeolite species is the anchoring interaction between the oxygen end of carbonyl ligands and the oxometal bonds, respectively, and the extraframework site-II Na^+ cations. The encapsulated

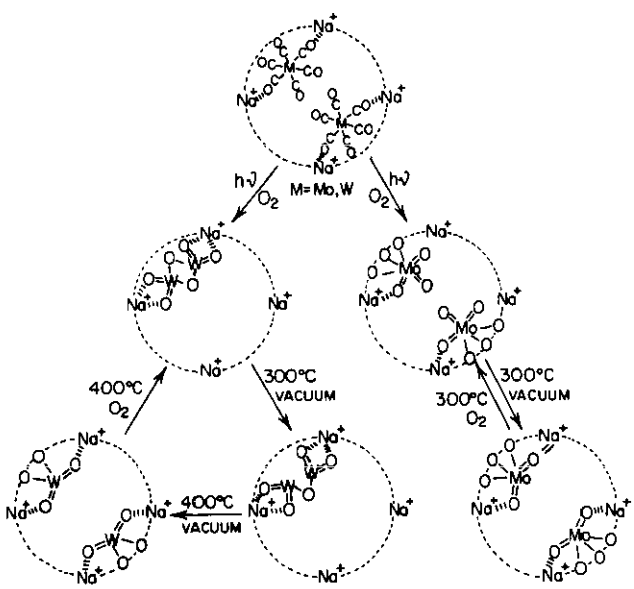

Figure 2. A schematic drawing of the intrazeolite structures and anchoring geometries of: $16\{Mo(CO)_6\}-Na_{56}Y$, $16\{MoO_3\}-Na_{56}Y$, $16\{MoO_2\}-Na_{56}Y$, $16\{W(CO)_6\}-Na_{56}Y$, $16\{WO_3\}-Na_{56}Y$, $16\{WO_{2.5}\}-Na_{56}Y$ and $16\{WO_2\}-Na_{56}Y$ [10–13].

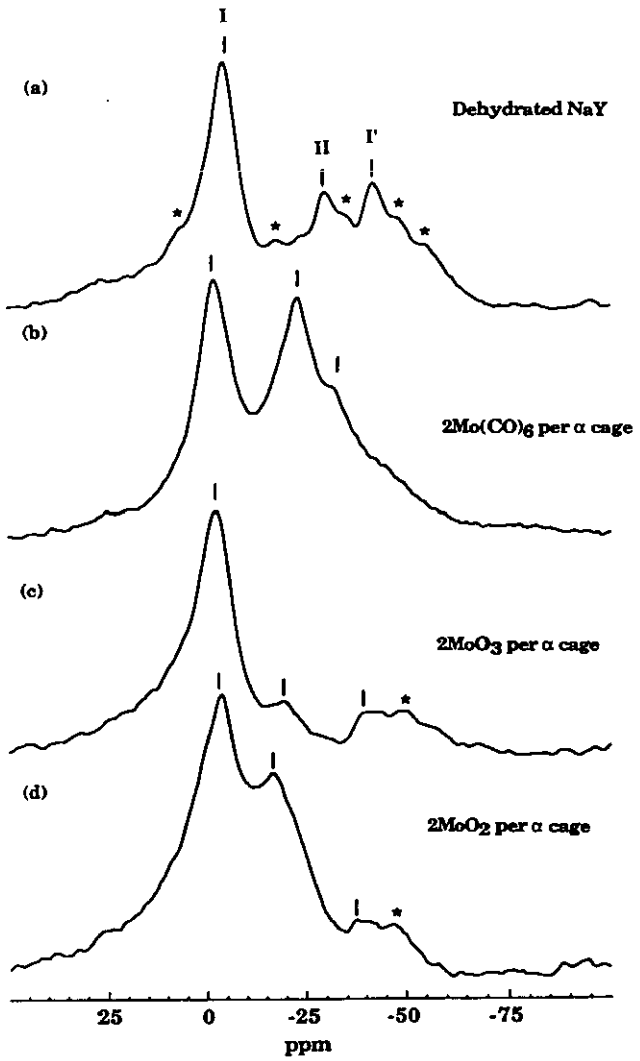

Figure 3. ^{23}Na-DOR spectra of (a) dehydrated $Na_{56}Y$ and $Na_{56}Y$ loaded with (b) $2Mo(CO)_6$ per α cage, (c) $2MoO_3$ per α cage and (d) $2MoO_2$ per α cage. * Indicates a spinning side band.

$16\{WO_{3-x}\}$–$Na_{56}Y$ materials, however, exhibit different structural features from those of the molybdenum oxide system, as shown in figure 2. Briefly, The $16\{WO_3\}$–$Na_{56}Y$ and $16\{WO_{2.5}\}$–$Na_{56}Y$ systems are viewed as supralattices of W_2O_6 and W_2O_5 dimers, respectively, while $16\{WO_2\}$–$Na_{56}Y$, $16\{MoO_3\}$–$Na_{56}Y$ and $16\{MoO_2\}$–$Na_{56}Y$ are considered to be supralattices of WO_2, MoO_3 and MoO_2 monomers, respectively. The tungsten oxide dimers are anchored to extraframework Na^+ cations whereas the molybdenum oxide monomers are bound primarily through the framework oxygens [10–13].

The NMR data shown in figures 3 and 4 support the proposed structural description and provide additional information. Anchoring of the encapsulated molybdenum complexes onto a particular extraframework cation site is shown in figure 3. A distinct ^{23}Na resonance, corresponding to sodium in α-cage site II, appears as $Mo(CO)_6$ molecules are inserted into the zeolite cavities, as shown in figure 3(b). The intensity of the other sodium resonances in the spectrum seems unaffected by the adsorption of $Mo(CO)_6$. Prior to the $Mo(CO)_6$ addition, a low-intensity site-II ^{23}Na DOR signal is observed, figure 3(a), since the Na^+ ions are not entirely localized at this particular site, which might be brought about by motion of the sodium cations within the α cage. This leads to a pronounced site distribution as well as high charge asymmetry at this sodium site, which causes a substantial broadening of the associated NMR spectral line [14]. The emergence of the intense sodium resonance at about −26 ppm as shown in figure 3(b), indicates the apparent formation of an assembly of intrazeolite $Mo(CO)_6$ molecules anchored to the accessible site-II sodium cations inside the α cages. The anchoring of the $Mo(CO)_6$ molecules, via the oxygen end of two trans-carbonyl ligands, to the site-II Na^+, binds the cations uniformly to the oxygen six-ring site inside the cavity, as well as creating a higher symmetry environment around the sodium nuclei.

$16\{MoO_3\}$–$Na_{56}Y$ and $16\{MoO_2\}$–$Na_{56}Y$ samples yield ^{23}Na DOR spectra which also feature signals due to Na^+ at site II, figures 3(c) and 3(d), although the respective resonances exhibit significantly different intensities. The change in the site-II Na^+ peak intensity might be a

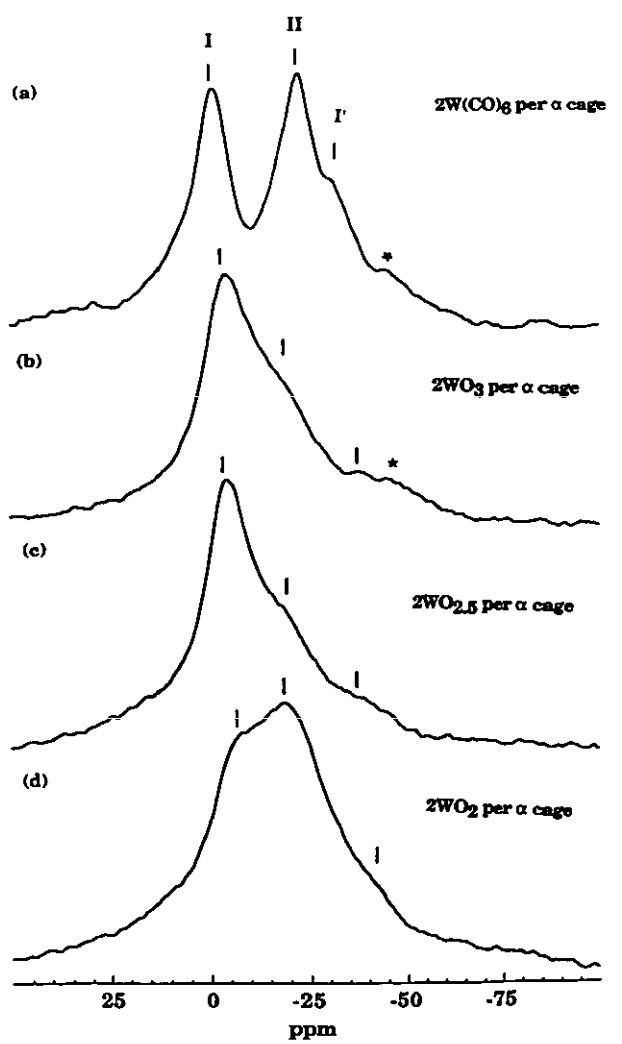

Figure 4. ^{23}Na-DOR spectra of $Na_{56}Y$ loaded with (a) $2W(CO)_6$ per α cage, and oxidation products (b) $2WO_3$ per α cage, (c) $2WO_{2.5}$ per α cage, and (d) $2WO_2$ per α cage. * Indicates a spinning side band.

consequence of the structural and symmetry changes that take place inside the α cage following the photooxidation of the $Mo(CO)_6$ precursor (figure 2). MoO_3 is considered to be a trigonal pyramidal monomer which is anchored essentially through three framework oxygens. The disposition of the oxometal bonds is such that one can interact with a single adjacent site-II Na^+ cation. On the other hand, both $Mo(CO)_6$ and MoO_2 have geometries that facilitate anchoring interactions to *two* site-II Na^+ cations. These ideas are illustrated in figure 2. Therefore, the site-II ^{23}Na DOR signal exhibits significantly higher intensity in $16\{Mo(CO)_6\}-Na_{56}Y$ and $16\{MoO_2\}-Na_{56}Y$ than in the $16\{MoO_3\}-Na_{56}Y$ sample, as shown in figure 3.

A similar intensity effect is detected in the ^{23}Na DOR spectra of the equivalent tungsten series, shown in figure 4. The DOR spectrum of $16\{W(CO)_6\}-Na_{56}Y$, figure 4(a), is almost identical to the $16\{Mo(CO)_6\}-Na_{56}Y$ spectrum, figure 3(b), indicating a similar arrangement of the guests in the two materials. The W_2O_6 dimer formed following the first photooxidation process is attached to *half* of the extraframework site-II Na^+ cations which were anchored to the carbonyl ligands of the parent $16\{W(CO)_6\}-Na_{56}Y$, figure 2. Indeed, the intensity of the corresponding α-cage site-II ^{23}Na diminishes substantially after the photooxidation stage, as shown in figure 4(b). The position of the anchoring sodium resonance shifts down-field in both oxidation products, $16\{WO_3\}-Na_{56}Y$ and $16\{WO_{2.5}\}-Na_{56}Y$ (figures 4(b) and (c), respectively), and appears as a shoulder to the main, down-field signal in the spectrum. These shifts indicate that the sodium environments differ significantly between the precursor material and the oxidation products. This difference can be traced to changes in anchoring geometry and strength between the oxygen end of a carbonyl ligand and an oxometal bond, with respect to the site-II Na^+ cation.

Following the final oxidation stage, WO_2 monomers are produced inside the zeolite cavities as shown in figure 2. The tungsten dioxide monomer, like the molybdenum analogue, has a secondary anchoring interaction with *two* site-II Na^+ cations through its two terminal oxygens. As each W_2O_6 dimer, anchored to two site-II Na^+ cations (figure 2), produces *two* WO_2 monomers upon thermal reductive-elimination of dioxygen, the effect in the ^{23}Na DOR spectrum is seen as a significant increase in the intensity of the resonance associated with the anchoring sodium nuclei, as shown in figure 4(d).

Higher loading of WO_2 guests did not have a significant effect upon the position and intensity of the signals in the ^{23}Na DOR spectrum [9]. This observation is consistent with the presence of essentially four site-II Na^+ cations within the α cage, which are already anchored in the $16\{WO_2\}-Na_{56}Y$ sample.

3. Conclusions

This study demonstrates the usefulness of high-resolution NMR, and in particular of the novel DOR technique, for providing chemical, structural and bonding details of a variety of guests in zeolite-Y. Issues addressed in this work included site-specific anchoring interactions, ordering, and structural changes of various metal carbonyl and molecular metal oxide guests within the α cages of $Na_{56}Y$ zeolite. Anchoring effects between the guests and site-II Na^+ extraframework cations are detected by ^{23}Na DOR, which provides information about the symmetry of the immediate environment and interaction strength of the binding sodium.

4. Experimental details

Preparation of the $n\{M(CO)_6\}-Na_{56}Y$ and $n\{MO_{3-x}\}-Na_{56}Y$ species is described elsewhere [10, 11]. The samples were packed in the DOR rotor under a dry argon atmosphere and the ^{23}Na experiments were conducted under rigorously anaerobic conditions. Double-rotation experiments were conducted in an 11.7 T magnetic field, using a Chemagnetics CMX-500 spectrometer. The features of the DOR probe have been described elsewhere [15]. The spinning speed was 5 kHz for the inner rotor and 600–800 Hz for the outer one. 1000–2000 acquisitions were accumulated in all NMR experiments, using short, 3 μs pulses with 0.5 s delays. The external reference was 0.1 M NaCl.

Acknowledgments

This work was supported by the Director, Office of Energy Research, Office of Basic Energy Sciences, Materials and Chemical Sciences Division, US Department of Energy under Contract No. DE-AC03-76SF00098. GAO wishes to acknowledge the Natural Science and Engineering Research Council (NSERC) of Canada's Operating and Strategic Grants Programmes. SO is grateful to the Chemistry Department, Middle East Technical University, for granting him an extended leave of absence to conduct this research at the University of Toronto.

References

[1] Reed M A and Kirk W P (ed) 1989 Nanostructure physics and fabrication *Proc. Int. Symp. College Station (Texas)* (New York: Academic)
[2] Stringfellow G B 1989 *Organometallic Vapor-Phase Epitaxy* (New York: Academic)
[3] Kroto H W, Heath J R, O'Brien S C, Curl R F and Smalley R E 1985 *Nature* **318** 162
[4] Wang Y and Mahler W 1987 *Opt. Commun.* **61** 233
[5] Zao X K, Baral S, Rolandi R, Fendler J H 1988 *J. Am. Chem. Soc.* **110** 1012
[6] Herron N, Wang Y, Eddy M M, Stucky G D, Cox D E, Moller K and Bein T 1989 *J. Am. Chem. Soc.* **111** 530
Ozin G A, Kuperman A and Stein A 1989 *Angew. Chem. Int. Ed. Adv. Mat.* **101** 373
Stucky G D and MacDougall J E 1990 *Science* **247** 663

[7] Wu Y, Chmelka B F, Pines A, Davis M E, Grobet P J and Jacobs P A 1990 *Nature* **346** 550
[8] Breck D W 1974 *Zeolite Molecular Sieves* (New York: Wiley)
[9] Jelinek R, Pines A, Özkar S and Ozin G A 1992 *J. Am. Chem. Soc.* at press
[10] Ozin G A and Özkar S 1990 *J. Phys. Chem.* **94** 7556
[11] Ozin G A, Malek A, Prokopowicz R, MacDonald P M, Özkar S, Moller K and Bein T 1991 Doping and band-gap engineering of an intrazeolite tungsten(VI) oxide supralattice *MRS Meeting (Anaheim, 1991)* Özkar S, Ozin G A and Prokopowicz R 1992 *J. Am. Chem. Soc.* submitted
[12] Ozin G A, Özkar S and MacDonald P M 1990 *J. Phys. Chem.* **94** 6939
[13] Moller K, Bein T, Özkar S and Ozin G A 1991 *J. Phys. Chem.* **95** 5276
[14] Mehring M 1983 *Principles of High Resolution NMR in Solids* (Berlin: Springer)
[15] Wu Y, Sun B Q, Pines A, Samoson A and Lippmaa E 1990 *J. Mag. Res.* **89** 297